

1 **Optimized pseudotyping conditions for the SARS-COV2 Spike glycoprotein**

2

3 Marc C. Johnson<sup>1\*</sup>, Terri D. Lyddon<sup>1</sup>, Reinier Suarez<sup>1</sup>, Braxton Salcedo<sup>1</sup>, Mary LePique<sup>1</sup>,

4 Maddie Graham<sup>1</sup>, Clifton Ricana<sup>1</sup>, Carolyn Robinson<sup>1</sup>, Detlef G. Ritter<sup>2</sup>

5

6 1 - Department of Molecular Microbiology and Immunology, University of Missouri-School of

7 Medicine, Christopher S. Bond Life Sciences Center, Columbia, MO

8 2 - Department of Anatomical and Clinical Pathology, MU Healthcare, Columbia, MO

9

10 Running Title: Pseudotyping SARS-COV2 Spike

11

12 \* Correspondence: [marcjohanson@missouri.edu](mailto:marcjohanson@missouri.edu) Tel.: 1-573-882-1519

13

14 **Abstract**

15 The SARS-COV2 Spike glycoprotein is solely responsible for binding to the host cell receptor  
16 and facilitating fusion between the viral and host membranes. The ability to generate viral  
17 particles pseudotyped with SARS-COV2 Spike is useful for many types of studies, such as  
18 characterization of neutralizing antibodies or development of fusion-inhibiting small molecules.  
19 Here we characterized the use of a codon-optimized SARS-COV2 Spike glycoprotein for the  
20 generation of pseudotyped HIV-1, MLV, and VSV particles. The full-length Spike protein  
21 functioned inefficiently with all three systems but was enhanced over 10-fold by deleting the last  
22 19 amino acids of the cytoplasmic tail of Spike. Infection of 293FT target cells was only  
23 possible if the cells were engineered to stably express the human ACE-2 receptor, but stably  
24 introducing an additional copy of this receptor did not further enhance susceptibility. Stable  
25 introduction of the Spike activating protease TMPRSS2 further enhanced susceptibility to  
26 infection by 5-10 fold. Substitution of the signal peptide of the Spike protein with an optimal  
27 signal peptide did not enhance or reduce infectious particle production. However, modification of  
28 a single amino acid in the furin cleavage site of Spike (R682Q) enhanced infectious particle  
29 production another 10-fold. With all enhancing elements combined, the titer of pseudotyped  
30 particles reached almost  $10^6$  infectious particles/ml. Finally, HIV-1 particles pseudotyped with  
31 SARS-COV2 Spike was successfully used to detect neutralizing antibodies in plasma from  
32 COVID-19 patients, but not plasma from uninfected individuals.

33

34 **Importance.**

35 When working with pathogenic viruses, it is useful to have rapid quantitative tests for viral  
36 infectivity that can be performed without strict biocontainment restrictions. A common way of  
37 accomplishing this is to generate viral pseudoparticles that contain the surface glycoprotein from  
38 the pathogenic virus incorporated into a replication-defective viral particle that contains a  
39 sensitive reporter system. These pseudoparticles enter cells using the glycoprotein from the

40 pathogenic virus leading to a readout for infection. Conditions that block entry of the pathogenic  
41 virus, such as neutralizing antibodies, will also block entry of the viral pseudoparticles.  
42 However, viral glycoproteins often are not readily suited for generating pseudoparticles. Here  
43 we describe a series of modifications that result in the production of relatively high titer SARS-  
44 COV2 pseudoparticles that are suitable for detection of neutralizing antibodies from COVID-19  
45 patients.

46

47 **Keywords:** SARS-COV2, COVID-19, pseudotypes, glycoprotein, lentiviral vector, neutralization  
48 assay

49

## 50 **Introduction**

51

52 The COVID-19 pandemic is a severe threat to human health and the global economy. COVID-  
53 19 is caused by infection with the SARS-CoV-2 virus, which is a highly pathogenic  
54 betacoronavirus (1, 2). A critical tool for the study of pathogenic viruses such as SARS-COV2 is  
55 a rapid and sensitive assay for agents that block viral entry such as neutralizing antibodies or  
56 small molecule inhibitors. A safe and powerful technique for generating such an assay is to  
57 generate viral pseudotyped particles where the surface fusion protein of the pathogen of interest  
58 is assembled onto the surface of replication-defective virus which contains a sensitive reporter  
59 protein.

60

61 The Spike glycoprotein from Coronaviruses facilitates binding to the host cell receptor and  
62 fusion between viral and cellular membranes. The SARS-COV2 Spike protein is a large 1,274  
63 amino acid protein that contains an N-terminal S1 receptor binding domain and a C-terminal S2  
64 fusion domain. Fusion by SARS-COV2 Spike requires binding to the host receptor ACE2 (3-6)  
65 as well as proteolytic cleavage by host proteases at the S1/S2 and S2' positions by host

66 cysteine proteases cathepsin B and L (CatB/L) or serine protease TMPRSS2 (3, 6). Depending  
67 on the cell line, inhibition of one or both of these proteases is sufficient to block viral entry. An  
68 interesting difference between the SARS-COV1 and COV2 Spike proteins is the presence of a  
69 furin cleavage site near the S1/S2 cleavage site (6, 7). This cleavage site was found to be  
70 essential for infection of human lung cells (3). Surprisingly, passaging of SARS-COV2 in Vero  
71 E6 cells selects for mutations that alter the furin cleavage site, resulting in virus that produce  
72 larger plaque sizes (8).

73  
74 There have been several reports generating SARS-COV1 (9-12) and SARS-COV2 (3-5, 13, 14)  
75 viral pseudotypes with glycoprotein-defective MLV, HIV, and VSV particles. Although  
76 pseudoparticles could be generated with full-length SARS-COV1 Spike, the pseudotyping  
77 efficiency was shown to be enhanced by about 100-fold by deleting the last 19 amino acids of  
78 the cytoplasmic tail (9) which removed a presumptive ER retention sequence. Mutation of the  
79 presumptive ER retention site in the cytoplasmic tail of SARS-COV2 (K1269A, H1271A) was not  
80 found to enhance pseudotyping efficiency (14). Here we develop optimized genetic conditions  
81 for generating a SARS-COV2 Spike pseudotyped particles.

82

## 83 **Results**

84 **Truncation of SARS-COV2 Spike enhances viral pseudotyping.** A codon optimized full  
85 length Spike gene was synthesized and introduced in place of the GFP gene in the plasmid  
86 pEGFP-N1. Because truncation of the cytoplasmic tail of SARS-COV1 Spike was shown to  
87 enhance production of viral pseudotypes (9), we also generated a SARS-COV2 Spike subclone  
88 with the last 19 amino acids deleted (Fig. 1). Pseudotyped particles were generated with the  
89 two Spike proteins as well as VSV-G with glycoprotein-defective MLV, HIV-1 and VSV particles  
90 (Fig. 1). To avoid potential false positive signal, a reporter system was utilized where the Cre  
91 recombinase gene is expressed by HIV-1 and MLV particles. When these particles transduce

92 the Cre reporter cell line, the protein causes a recombination in an engineered reporter element  
93 that results in GFP expression. Because the viral producing cells do not express GFP, they are  
94 eliminated as a source of false positive signal. This 293FT based reporter cell line was further  
95 engineered to express human ACE2. Infectious particle production with all three types of  
96 particles was very low with the full-length Spike protein, but the  $\Delta 19$  Spike produced viral titers  
97 approaching  $10^4$  infectious particles/ml with both HIV-1 and VSV particles. The infectious  
98 particle production remained over 1000-fold lower than with the control glycoprotein, VSV-G.

99 To allow rapid quantitation with minimum background, we proceeded with an Env-  
100 defective HIV-1 provirus containing a *gaussia* luciferase (Gluc) gene in the reverse orientation  
101 containing a forward intron (Fig. 2 (15)). This viral construct produces very low background  
102 because it is not capable of producing luciferase signal unless the gene is reverse transcribed in  
103 the target cell. Infectivity with SARS-COV2 Spike requires expression of the host receptor  
104 ACE2. Our starting cell line was generated using a retroviral transfer vector containing ACE2  
105 and a puromycin selection cassette. To determine if introduction of an additional stable copy of  
106 ACE2 would enhance susceptibility to infection, we generated a second retroviral transfer vector  
107 with a blasticidin resistance cassette. Retroviral particles were generated with this vector and  
108 used to stably transduce 293FT or 293FT/ACE2 (puro) cells. Each of the cell lines was  
109 transduced with HIV-1-Gluc particles pseudotyped with SARS-COV2  $\Delta 19$  Spike (Fig. 2). As  
110 expected, 293FT cells were not susceptible to infection with the HIV-1/SARS-COV2  $\Delta 19$  Spike.  
111 However, both cell lines containing a single introduction of ACE2, and the cell line containing  
112 two introductions had approximately 1000-fold increase in luciferase signal, but the signal was  
113 roughly equivalent among the three cell lines.

114 **TMPRSS2 expression enhances susceptibility of cells to SARS-COV2 pseudotypes.** The  
115 SARS-COV2 Spike requires proteolytic priming during infection by either cysteine proteases  
116 CatB/L or serine protease TMPRSS2 produced in the target cell (3, 6). To determine whether

117 introduction of TMPRSS2 would enhance susceptibility to infection, we synthesized a codon-  
118 optimized TMPRSS2 gene, introduced this gene into a retroviral transfer vector, and stably  
119 transduced 293FT or 293FT/ACE2 cells. The stable introduction of TMPRSS2 to 293FT cells  
120 did not impart sensitivity to transduction with HIV-1 particles pseudotyped with SARS-COV2  $\Delta$ 19  
121 Spike (Fig. 3). However, stable introduction of TMPRSS2 to 293FT/ACE2 cells increased the  
122 Gluc signal from target cells by 5-10 fold. Neither ACE2 expression nor TMPRSS2 expression  
123 affected Gluc signal from particles pseudotyped with VSV-G.

124 **The R682Q mutation in SARS-COV2 Spike enhances pseudotyping efficiency.** To explore  
125 additional genetic modifications in SARS-COV2 that might enhance infectious particle  
126 production, we replaced the endogenous signal peptide with a well characterized strong signal  
127 peptide (16), and separately we introduced a point mutation in the furin-cleavage site of SARS-  
128 COV2  $\Delta$ 19 Spike (R682Q) that has previously been reported to increase SARS-COV2 plaque  
129 sizes (Fig. 4 (8)). Infectious particle production was assessed using both Gluc and Cre  
130 reporters, and transductions were performed in cell lines with and without TMPRSS2. To  
131 minimize target cell variation, the transductions were all performed in 293FT/Cre-reporter/ACE2  
132 and 293FT/Cre-reporter/ACE2/TMPRSS2 cells. Replacement of the signal peptide did not  
133 increase or decrease infectious particle production (Fig 4A). However, the R682Q mutation  
134 significantly enhanced infectious particle production under all conditions. The enhancement  
135 was most pronounced with virus containing the Cre reporter in cells lacking TMPRSS2 (11-fold).  
136 The highest titer of  $8 \times 10^5$  was achieved with the R682Q  $\Delta$ 19 Spike into cells expressing both  
137 ACE2 and TMPRSS2.

138 **SARS-COV2 Spike pseudotypes function in neutralization assays.** To test if the  
139 pseudoparticles produced were suitable for use in a neutralization assay, we incubated HIV-1  
140 particles pseudotyped with SARS-COV2  $\Delta$ 19 Spike with and without the R682Q mutation with  
141 serial dilutions of control plasma and plasma from COVID-19 patients before adding

142 293FT/ACE2/TMPRSS2 cells. Robust and quantifiable neutralization was detected in plasma  
143 from COVID-19 plasma, but not from control plasma. The R682Q mutation did not noticeably  
144 affect sensitivity to neutralizing antibodies.

145

146

147

## 148 **Methods.**

149

150 **Plasmids.** The gammaretroviral transfer plasmids pQCXIP (puromycin resistance) and  
151 pQCXIH (pygromycin resistance) were obtained from Clontech. The blasticidin gammaretroviral  
152 transfer vector (pQCXIB) was generated by replacing the puromycin resistance cassette from  
153 PQCXIP with a blasticidin resistance cassette. The gammaretroviral vector for generating the  
154 Cre sensor cell line (MLV lox-mTomato-lox-GFP-Blast) was engineered into pQCXIB and  
155 contained the monomeric Tomato gene flanked by Lox sequences  
156 (ATAACTTCGTATAGCATACATTATACGAAGTTAT), which was followed immediately by  
157 eGFP. The ACE2 transfer vectors were generated by engineering the human ACE2 gene  
158 (NCBI Reference Sequence: NM\_021804.3) into pQCXIP and pQCXIH. The TMPRSS2  
159 transfer vector was generated by synthesizing a codon-optimized version of the human  
160 TMPRSS2 gene (NCBI Reference Sequence: NP\_001128571.1) and engineering it into the  
161 vector pQCXIH. The HIV-1-CMV-Cre vector was an NL4-3 derived provirus that is defective in  
162 Vif, Vpr, Env and has the Nef gene replaced with CMV-Cre. The plasmid was generated by  
163 replacing the GFP gene from the previously described plasmid HIV-CMV-GFP+Vpu (17) with  
164 the Cre gene from plasmid MLV-Cre (18), provided by Alan Rein (NCI Frederick). The MLV+  
165 CMV Cre vector was generated by replacing the GFP gene from MLV-GFP (provided by Shan-  
166 Lu Liu, The Ohio State University) with the Cre gene from MLV-Cre (18), provided by Alan Rein  
167 (NCI Frederick). The MLV GagPol expression construct was provided by Walther Mothes (Yale

168 University). The HIV-1-Gluc vector was previously described (19). The VSV-G expression  
169 construct was obtained from the NIH AIDS Reagent Program (20). The SARS-COV2  
170 expression vector was generated by synthesizing a codon-optimized version of the SARS-  
171 COV2 Spike (GenBank accession number MN985325.1). The  $\Delta$ 19 Spike and the  $\Delta$ 19 R682Q  
172 Spike were generated by PCR mutagenesis. The Spike subclone with the alternative signal  
173 peptide contained the previously described H7 peptide (16) was generated by synthesizing the  
174 5' end of the Spike gene with the alternative signal peptide and introducing it into the SARS-  
175 COV2  $\Delta$ 19 Spike clone.

176  
177 **Virus production and infectivity assays.** All transfections were performed in 6 well plates.  
178 293FT cells were transfected with a total of 1 microgram of plasmid and 4 micrograms of PEI  
179 (21). For HIV-1-CMV-Cre particles, cells were transfected with 900ng of provirus and 100ng of  
180 glycoprotein expression vector in Fig. 1, and 800ng of provirus and 200ng of glycoprotein  
181 expression vector in subsequent figures. For HIV-1-Gluc particles, cells were transfected with  
182 800ng of provirus and 200ng of glycoprotein expression vector. For MLV particles, cells were  
183 transfected with 500ng of MLV GagPol expression vector, 400ng of MLV-CMV-Cre, and 100ng  
184 of glycoprotein expression vector. For VSV particles, cells were transfected with 1 microgram of  
185 glycoprotein expression, and were infected 2 days post-transfection with  $>10^7$  infectious  
186 units/well of VSV $\Delta$ G-GFP (Kerafast, (22)). Cells were rinsed with PBS one hour after infection  
187 and replace with complete media supplemented with 2 microliters of mouse hybridoma  
188 supernatant containing anti-VSV-G antibody I1 (Kerafast) to neutralize input virus. Neutralizing  
189 anti-body was excluded from samples pseudotyped with VSV-G. VSV pseudoparticles were  
190 collected 24 hours later.

191 Supernatant containing virus was frozen at  $-80^{\circ}\text{C}$  for at least 4 h, thawed, and spun at  
192 3,200 x g for 5 min, and the same volume of medium was added to target cells with 20



193 micrograms of hexadimethrine bromide per ml (H9268; Sigma). For assays with a fluorescent  
194 readout, infected cells were collected at about 2-3 days post-infection, fixed with 4%  
195 paraformaldehyde, washed with phosphate-buffered saline (PBS), and analyzed on an Accuri  
196 C6 flow cytometer. For infections with a Gluc readout, transductions were allowed to proceed  
197 for 2-3 days and 20 microliters of supernatant from each well was transferred to a black 96-well  
198 plate for measuring *Gaussia* luciferase activity with 50 microliters of 10 micromolar  
199 coelenterazine in 0.1 M Tris (pH 7.4) and 0.3 M sodium ascorbate (NanoLight Technology).  
200 Luminescence, representing infectivity, was measured from the supernatant using a  
201 PerkinElmer Enspire 2300 Multilabel Reader.

202 **Cell culture.** The 293FT cell line was obtained from Invitrogen. All cells were maintained in  
203 Dulbecco's modified Eagle's medium (DMEM) supplemented with 10% fetal bovine serum, 2  
204 mM L-glutamine, 1 mM sodium pyruvate, 10 mM nonessential amino acids, and 1% minimal  
205 essential medium (MEM) vitamins.

206 **Cell line generation.** The Cre sensor cell line was generated by transfecting 293FT cells with  
207 500 ng MLV GagPol expression vector, 400 ng of retroviral transfer vector MLV lox-mTomato-  
208 lox-GFP-Blast, and 100 ng of VSV-G expression vector. Viral media was used to transduce  
209 293FT cells, and cells were selected with blasticidin (5 micrograms/ml) beginning 2 days post-  
210 transduction and maintained until control treated cells were all eliminated. A clonal isolate from  
211 these cells was selected that expressed mTomato but no GFP. The ACE2 cell lines were  
212 generated by transfecting 293FT cells with 500 ng MLV GagPol expression vector, 400 ng of  
213 retroviral transfer vector pQCXIP-ACE2 or pQCXIH-ACE2, and 100 ng of VSV-G expression  
214 vector. Viral media was used to transduce 293FT cells or the 293FT sensor cell line, and cells  
215 were selected with puromycin (1 microgram/ml) or hygromycin (200 micrograms/ml) beginning 2  
216 days post-transduction and maintained until control treated cells were all eliminated. The  
217 TMPRSS2 cell line was generated by transfecting 293FT cells with 500 ng MLV GagPol

218 expression vector, 400 ng of retroviral transfer vector pQCXIH-TMPRSS2, and 100 ng of VSV-G  
219 expression vector. Viral media was used to transduce 293FT, 293FT/ACE2, or 293/Cre-  
220 sensor/ACE2 cells were selected with hygromycin (200 micrograms/ml) beginning 2 days post-  
221 transduction and maintained until control treated cells were all eliminated.

222 **Neutralization assay.** Deidentified patient plasma samples were obtained from the clinical  
223 laboratory MU healthcare. Plasma was heat-inactivated for 30 minutes at 58C. Two-fold  
224 serially diluted plasma was incubated with HIV-1/SARS-COV2 Spike pseudotypes for 1 hour at  
225 37C. The mixture was subsequently incubated with 293/ACE2/TMPRSS2 cells, approximately  
226 20,000 cells per well in a 96 well plate. Gluc measurements were taken 2-3 days post  
227 transduction.

## 228 **Discussion.**

229 Here we outline glycoprotein and target cell modifications that enhance pseudotyping  
230 efficiency with the SARS-COV2 Spike glycoprotein. The first and most important changes are  
231 the necessity to express the human ACE2 receptor, which has been defined previously by  
232 numerous investigators, and the enhancement gained from truncation of the Spike cytoplasmic  
233 tail. Truncation of the last 19 amino acids for SARS-COV1 was also shown to significantly  
234 enhance pseudotyping with that glycoprotein (9). In that study, the original reason for making  
235 the truncation was to eliminate potential ER retention sequences in the cytoplasmic tail. Despite  
236 enhancing pseudotyping capacity, the truncation did not enhance surface expression. It is likely  
237 that the enhancement in pseudotyping efficiency upon deletion of the cytoplasmic is at least in  
238 part due to eliminating steric interference of the cytoplasmic tail with the viral capsid. Such  
239 interference has been noted when pseudotyping other viral glycoproteins with large cytoplasmic  
240 tails, such as HIV-1 Env (23, 24).

241           The next modification that enhanced efficiency was the introduction of the human  
242 protease TMPRSS2. The importance of this protease for SARS-COV2 Spike glycoprotein entry  
243 has been noted previously, so this enhancement was not surprising (3, 6).

244           The final modification that enhanced SARS-COV2  $\Delta$ 19 Spike pseudotyping was the  
245 introduction of the R682Q mutation, which is predicted to eliminate the furin cleavage site. This  
246 mutation was naturally selected for upon culturing SARS-COV2 in Vero cells, and viruses  
247 containing the mutation were reported to have larger plaque sizes (8). This observation is  
248 slightly at odds with a recent publication by Hoffmann et al. that found that the furin cleavage  
249 site was essential for infecting the lung cell line Calu-3, but not Vero cells. The Calu-3 cell line  
250 is reported to express TMPRSS2, but lack sufficient CatB/L to promote glycoprotein priming (3,  
251 25); the Vero cells are reported to be TMPRSS2 negative, but CatB/L positive. Thus, the furin  
252 cleavage site appeared to only be required when the virus is dependent on TMPRSS2 for entry.  
253 A possible explanation is that furin cleavage enhances TMPRSS2 mediated entry, but  
254 suppresses CatB/L mediated entry. Consistent with this, the enhancement we observed from  
255 the R682Q mutation was less pronounced in cells that express TMPRSS2. It should be noted  
256 that mutations described in Hoffman et al. replaced the furin cleavage site from SARS-COV2  
257 with the equivalent sequence from SARS-COV1, which effectively causes a 4 amino acid  
258 deletion. Thus, the loss of infectivity observed by Hoffmann et al. could in part have been the  
259 result secondary effects of the deletion that is independent of furin cleavage.

260           Finally, we demonstrate that HIV-1-Gluc particles pseudotyped with SARS-COV2  $\Delta$ 19  
261 Spike could be used for detecting neutralizing antibodies from COVID-19 patient plasma.  
262 Inclusion of the R682Q in Spike did not obviously change the neutralization results in this assay.  
263 Thus, this appears to be a suitable system for studying inhibitors of SARS-COV2 entry.

264

265 **References**

266

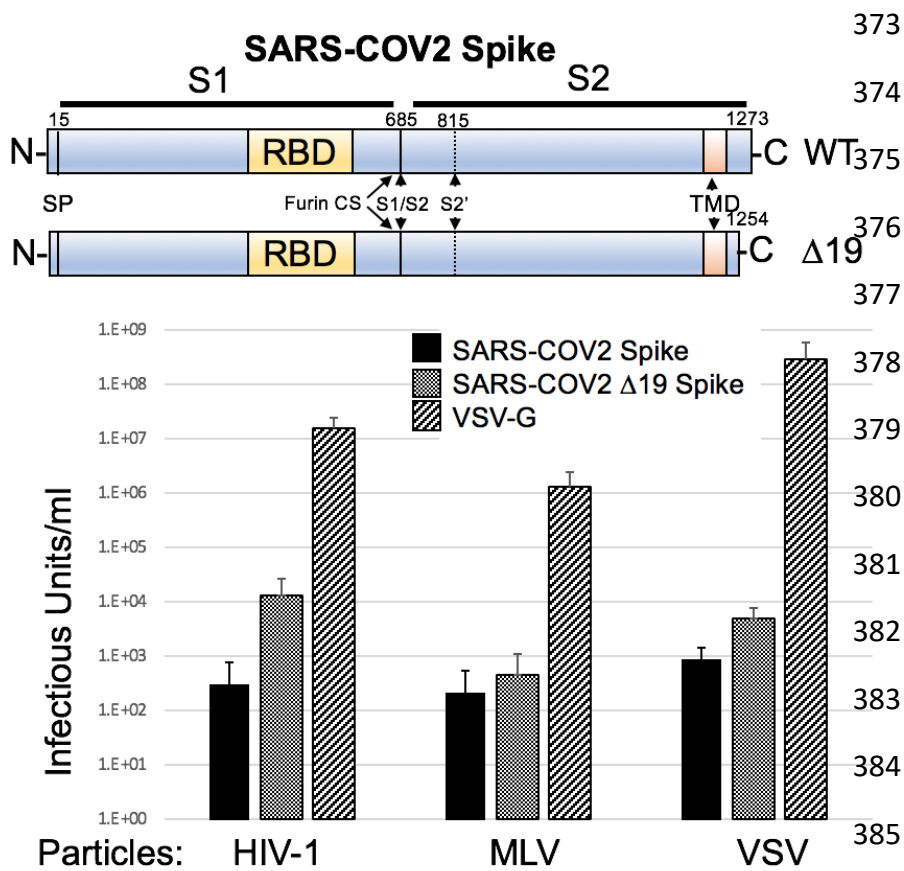
- 267 1. Zhu N, Zhang D, Wang W, Li X, Yang B, Song J, Zhao X, Huang B, Shi W, Lu R, Niu P, Zhan  
268 F, Ma X, Wang D, Xu W, Wu G, Gao GF, Tan W, China Novel Coronavirus I, Research T. A Novel  
269 Coronavirus from Patients with Pneumonia in China, 2019. *The New England journal of*  
270 *medicine*. 2020;382(8):727-33. Epub 2020/01/25. doi: 10.1056/NEJMoa2001017. PubMed  
271 PMID: 31978945; PMCID: PMC7092803.
- 272 2. Zhou P, Yang XL, Wang XG, Hu B, Zhang L, Zhang W, Si HR, Zhu Y, Li B, Huang CL, Chen  
273 HD, Chen J, Luo Y, Guo H, Jiang RD, Liu MQ, Chen Y, Shen XR, Wang X, Zheng XS, Zhao K, Chen  
274 QJ, Deng F, Liu LL, Yan B, Zhan FX, Wang YY, Xiao GF, Shi ZL. A pneumonia outbreak associated  
275 with a new coronavirus of probable bat origin. *Nature*. 2020;579(7798):270-3. Epub  
276 2020/02/06. doi: 10.1038/s41586-020-2012-7. PubMed PMID: 32015507; PMCID:  
277 PMC7095418.
- 278 3. Hoffmann M, Kleine-Weber H, Schroeder S, Kruger N, Herrler T, Erichsen S, Schiergens  
279 TS, Herrler G, Wu NH, Nitsche A, Muller MA, Drosten C, Pohlmann S. SARS-CoV-2 Cell Entry  
280 Depends on ACE2 and TMPRSS2 and Is Blocked by a Clinically Proven Protease Inhibitor. *Cell*.  
281 2020;181(2):271-80 e8. Epub 2020/03/07. doi: 10.1016/j.cell.2020.02.052. PubMed PMID:  
282 32142651; PMCID: PMC7102627.
- 283 4. Letko M, Marzi A, Munster V. Functional assessment of cell entry and receptor usage for  
284 SARS-CoV-2 and other lineage B betacoronaviruses. *Nat Microbiol*. 2020;5(4):562-9. Epub  
285 2020/02/26. doi: 10.1038/s41564-020-0688-y. PubMed PMID: 32094589; PMCID:  
286 PMC7095430.
- 287 5. Ou X, Liu Y, Lei X, Li P, Mi D, Ren L, Guo L, Guo R, Chen T, Hu J, Xiang Z, Mu Z, Chen X,  
288 Chen J, Hu K, Jin Q, Wang J, Qian Z. Characterization of spike glycoprotein of SARS-CoV-2 on  
289 virus entry and its immune cross-reactivity with SARS-CoV. *Nat Commun*. 2020;11(1):1620.  
290 Epub 2020/03/30. doi: 10.1038/s41467-020-15562-9. PubMed PMID: 32221306; PMCID:  
291 PMC7100515.
- 292 6. Walls AC, Park YJ, Tortorici MA, Wall A, McGuire AT, Veasley D. Structure, Function, and  
293 Antigenicity of the SARS-CoV-2 Spike Glycoprotein. *Cell*. 2020;181(2):281-92 e6. Epub  
294 2020/03/11. doi: 10.1016/j.cell.2020.02.058. PubMed PMID: 32155444; PMCID: PMC7102599.
- 295 7. Wrapp D, Wang N, Corbett KS, Goldsmith JA, Hsieh CL, Abiona O, Graham BS, McLellan  
296 JS. Cryo-EM structure of the 2019-nCoV spike in the prefusion conformation. *Science*.  
297 2020;367(6483):1260-3. Epub 2020/02/23. doi: 10.1126/science.abb2507. PubMed PMID:  
298 32075877; PMCID: PMC7164637.
- 299 8. Ogando NS, Dalebout TJ, Zevenhoven-Dobbe JC, Limpens RW, van der Meer Y, Caly L,  
300 Druce J, de Vries JJC, Kikkert M, Bárcena M, Sidorov I, Snijder EJ. SARS-coronavirus-2 replication  
301 in Vero E6 cells: replication kinetics, rapid adaptation and cytopathology. *BioRx (Preprint)*.  
302 2020. doi: <https://doi.org/10.1101/2020.04.20.049924>.
- 303 9. Girolglou T, Cinatl J, Jr., Rabenau H, Drosten C, Schwalbe H, Doerr HW, von Laer D.  
304 Retroviral vectors pseudotyped with severe acute respiratory syndrome coronavirus S protein. *J*  
305 *Virol*. 2004;78(17):9007-15. Epub 2004/08/17. doi: 10.1128/JVI.78.17.9007-9015.2004. PubMed  
306 PMID: 15308697; PMCID: PMC506966.

- 307 10. Han DP, Kim HG, Kim YB, Poon LL, Cho MW. Development of a safe neutralization assay  
308 for SARS-CoV and characterization of S-glycoprotein. *Virology*. 2004;326(1):140-9. Epub  
309 2004/07/21. doi: 10.1016/j.virol.2004.05.017. PubMed PMID: 15262502; PMCID: PMC7127165.
- 310 11. Simmons G, Reeves JD, Rennekamp AJ, Amberg SM, Piefer AJ, Bates P. Characterization  
311 of severe acute respiratory syndrome-associated coronavirus (SARS-CoV) spike glycoprotein-  
312 mediated viral entry. *Proc Natl Acad Sci U S A*. 2004;101(12):4240-5. Epub 2004/03/11. doi:  
313 10.1073/pnas.0306446101. PubMed PMID: 15010527; PMCID: PMC384725.
- 314 12. Yang ZY, Huang Y, Ganesh L, Leung K, Kong WP, Schwartz O, Subbarao K, Nabel GJ. pH-  
315 dependent entry of severe acute respiratory syndrome coronavirus is mediated by the spike  
316 glycoprotein and enhanced by dendritic cell transfer through DC-SIGN. *J Virol*.  
317 2004;78(11):5642-50. Epub 2004/05/14. doi: 10.1128/JVI.78.11.5642-5650.2004. PubMed  
318 PMID: 15140961; PMCID: PMC415834.
- 319 13. Ni L, Ye F, Cheng ML, Feng Y, Deng YQ, Zhao H, Wei P, Ge J, Gou M, Li X, Sun L, Cao T,  
320 Wang P, Zhou C, Zhang R, Liang P, Guo H, Wang X, Qin CF, Chen F, Dong C. Detection of SARS-  
321 CoV-2-Specific Humoral and Cellular Immunity in COVID-19 Convalescent Individuals. *Immunity*.  
322 2020. Epub 2020/05/16. doi: 10.1016/j.immuni.2020.04.023. PubMed PMID: 32413330; PMCID:  
323 PMC7196424.
- 324 14. Crawford KHD, Eguia R, Dingens AS, Loes AN, Malone KD, Wolf CR, Chu HY, Tortorici MA,  
325 Vesler D, Murphy M, Pettie D, King NP, Balazs AB, Bloom JD. Protocol and Reagents for  
326 Pseudotyping Lentiviral Particles with SARS-CoV-2 Spike Protein for Neutralization Assays.  
327 *Viruses*. 2020;12(5). Epub 2020/05/10. doi: 10.3390/v12050513. PubMed PMID: 32384820.
- 328 15. Janaka SK, Gregory DA, Johnson MC. Retrovirus glycoprotein functionality requires  
329 proper alignment of the ectodomain and the membrane proximal cytoplasmic tail. *J Virol*. 2013.  
330 Epub 2013/09/21. doi: 10.1128/JVI.01847-13. PubMed PMID: 24049172.
- 331 16. Haryadi R, Ho S, Kok YJ, Pu HX, Zheng L, Pereira NA, Li B, Bi X, Goh LT, Yang Y, Song Z.  
332 Optimization of heavy chain and light chain signal peptides for high level expression of  
333 therapeutic antibodies in CHO cells. *PLoS One*. 2015;10(2):e0116878. Epub 2015/02/24. doi:  
334 10.1371/journal.pone.0116878. PubMed PMID: 25706993; PMCID: PMC4338144.
- 335 17. Lucas TM, Lyddon TD, Cannon PM, Johnson MC. Pseudotyping incompatibility between  
336 HIV-1 and gibbon ape leukemia virus Env is modulated by Vpu. *J Virol*. 2010;84(6):2666-74.  
337 Epub 2010/01/01. doi: JVI.01562-09 [pii]  
338 10.1128/JVI.01562-09. PubMed PMID: 20042505; PMCID: 2826068.
- 339 18. Ahi YS, Zhang S, Thappeta Y, Denman A, Feizpour A, Gummuluru S, Reinhard B, Muriaux  
340 D, Fivash MJ, Rein A. Functional Interplay Between Murine Leukemia Virus Glycogag, Serinc5,  
341 and Surface Glycoprotein Governs Virus Entry, with Opposite Effects on Gammaretroviral and  
342 Ebolavirus Glycoproteins. *mBio*. 2016;7(6). Epub 2016/11/24. doi: 10.1128/mBio.01985-16.  
343 PubMed PMID: 27879338; PMCID: PMC5120145.
- 344 19. Janaka SK, Lucas TM, Johnson MC. Sequences in gibbon ape leukemia virus envelope  
345 that confer sensitivity to HIV-1 accessory protein Vpu. *J Virol*. 2011;85(22):11945-54. Epub  
346 2011/09/16. doi: 10.1128/JVI.05171-11. PubMed PMID: 21917962; PMCID: 3209308.
- 347 20. Chang LJ, Urlacher V, Iwakuma T, Cui Y, Zucali J. Efficacy and safety analyses of a  
348 recombinant human immunodeficiency virus type 1 derived vector system. *Gene Therapy*.  
349 1999;6(5):715-28.

- 350 21. Boussif O, Lezoualc'h F, Zanta MA, Mergny MD, Scherman D, Demeneix B, Behr JP. A  
351 versatile vector for gene and oligonucleotide transfer into cells in culture and in vivo:  
352 polyethylenimine. *Proc Natl Acad Sci U S A*. 1995;92(16):7297-301. Epub 1995/08/01. PubMed  
353 PMID: 7638184; PMCID: 41326.
- 354 22. Whitt MA. Generation of VSV pseudotypes using recombinant DeltaG-VSV for studies on  
355 virus entry, identification of entry inhibitors, and immune responses to vaccines. *J Virol*  
356 *Methods*. 2010;169(2):365-74. Epub 2010/08/17. doi: 10.1016/j.jviromet.2010.08.006. PubMed  
357 PMID: 20709108; PMCID: PMC2956192.
- 358 23. Mammano F, Salvatori F, Indraccolo S, De Rossi A, Chieco-Bianchi L, Gottlinger HG.  
359 Truncation of the human immunodeficiency virus type 1 envelope glycoprotein allows efficient  
360 pseudotyping of Moloney murine leukemia virus particles and gene transfer into CD4+ cells. *J*  
361 *Virol*. 1997;71(4):3341-5. PubMed PMID: 9060707.
- 362 24. Schnierle BS, Stitz J, Bosch V, Nocken F, Merget-Millitzer H, Engelstadter M, Kurth R,  
363 Groner B, Cichutek K. Pseudotyping of murine leukemia virus with the envelope glycoproteins  
364 of HIV generates a retroviral vector with specificity of infection for CD4-expressing cells.  
365 *Proceedings of the National Academy of Sciences of the United States of America*.  
366 1997;94(16):8640-5.
- 367 25. Park JE, Li K, Barlan A, Fehr AR, Perlman S, McCray PB, Jr., Gallagher T. Proteolytic  
368 processing of Middle East respiratory syndrome coronavirus spikes expands virus tropism. *Proc*  
369 *Natl Acad Sci U S A*. 2016;113(43):12262-7. Epub 2016/10/30. doi: 10.1073/pnas.1608147113.  
370 PubMed PMID: 27791014; PMCID: PMC5086990.

371

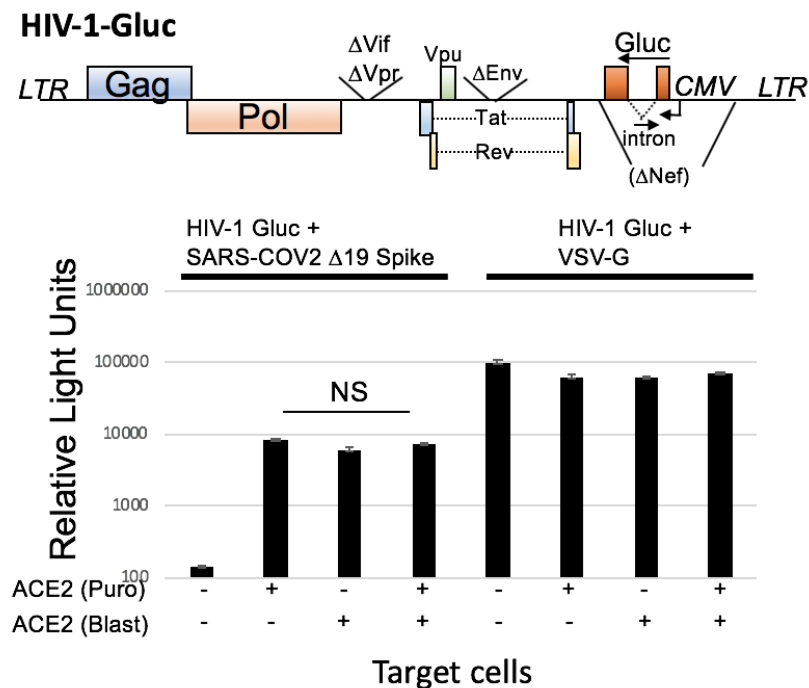
372



386

387 **Figure 1.** SARS-COV2 pseudotyped particles. Upper, schematic of SARS-COV2 Spike  
388 protein. RBD = receptor binding domain, SP = signal peptide, TMD = transmembrane domain,  
389 furin CS = furin cleavage site. Lower, infectious particle production of glycoprotein defective  
390 HIV-1, MLV, or VSV pseudoparticles with SARS-COV2 Spike, SARS-COV2  $\Delta 19$  Spike, and  
391 VSV-G. HIV-1 and MLV particles contained a Cre reporter and were scored on 293FT/ACE2  
392 cells containing a Cre-inducible GFP reporter. VSV-G particles directly contained GFP (VSV $\Delta$ G-  
393 GFP). Data are the average and standard deviation of three independent experiments.





394

395 **Figure 2. Introduction of ACE2 is required for infection of 293FT cells with SARS-COV2**

396 **Spike.** Upper, schematic of the HIV-1 *gussia* luciferase vector. Lower, transduction of 293FT

397 cells transduced with different numbers of ACE2 genes with HIV-1-Gluc pseudoparticles

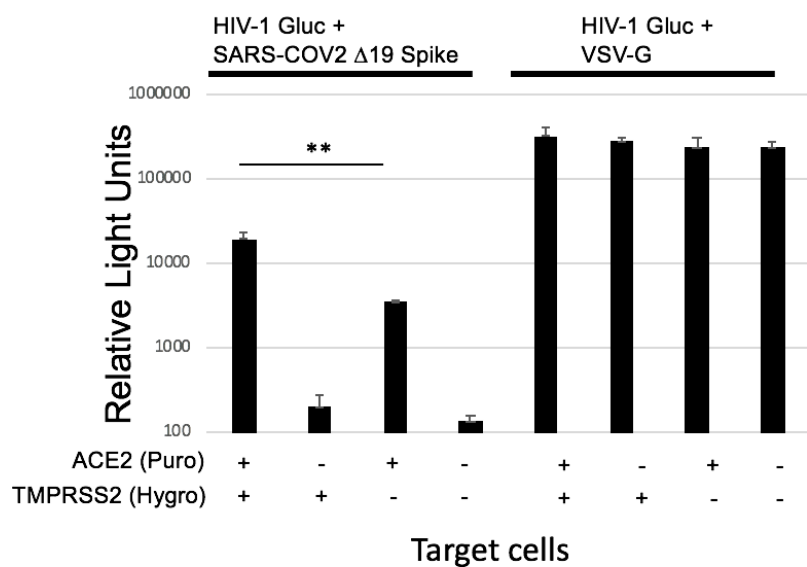
398 pseudotyped with SARS-COV2  $\Delta$ 19 Spike or VSV-G. Transductions with VSV-G used 100-

399 times less viral supernatant. Data are the average and standard deviation of a representative

400 experiment performed in triplicate. NS = no significant difference.

401





402

403

404 **Figure 3. TMPRSS2 expression enhances susceptibility to infection with SARS-COV2**

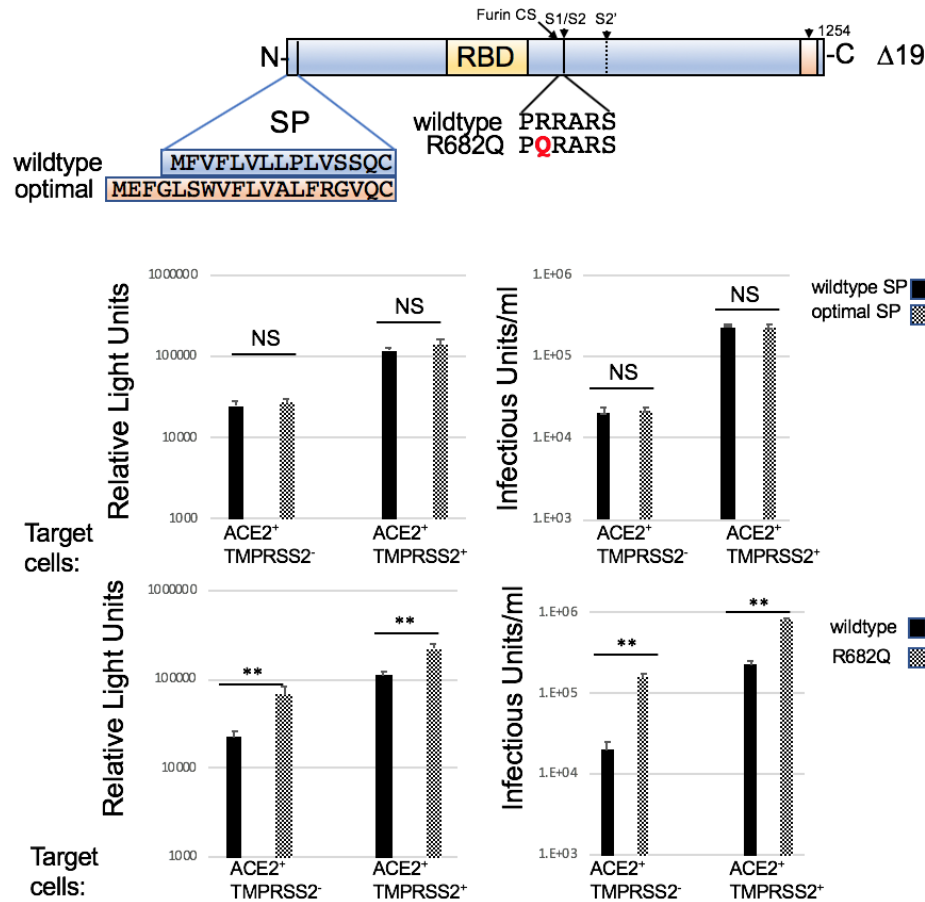
405 **Spike.** 293FT cells stably expressing ACE2, TMPRSS2, or both were transduced with HIV-1-

406 Gluc particles pseudotyped with SARS-COV2 Δ19 Spike or VSV-G. Transductions with VSV-G

407 used 100-times less viral supernatant. Data are the average and standard deviation of a

408 representative experiment performed in triplicate. \*\* p<0.01 in paired Student's t-test.

409



410

411

412

413 **Figure 4. R682 mutation in SARS-COV2 Δ19 Spike enhances pseudotyping.** Upper,

414 schematic illustrating introduction of the optimal SP and R682Q into SARS-COV2 Δ19 Spike.

415 HIV-1-GLuc and HIV-CMV-Cre were pseudotyped with SARS-COV2 Δ19 Spike, SARS-COV2

416 Δ19 Spike with optimal SP, and SARS-COV2 R682Q Δ19 Spike. Transductions were

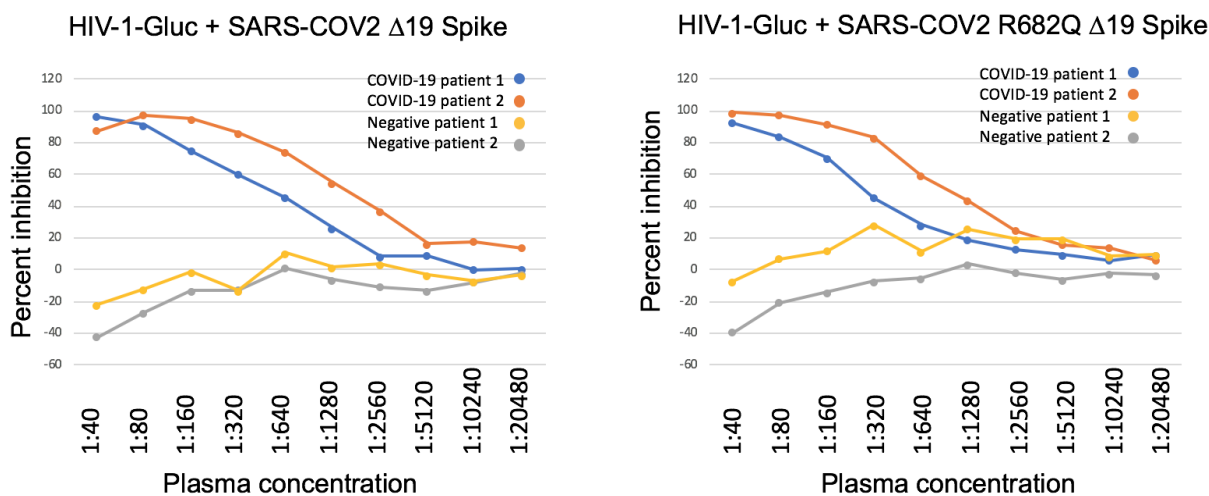
417 performed on 293FT/ACE2 and 293FT/ACE2/TMPRSS2 cells both containing a Cre-inducible

418 GFP reporter. Data are the average and standard deviation of a representative experiment

419 performed in triplicate. NS = no significant difference., \*\* p<0.01 in paired Student's t-test.

420

421



422 **Figure 5. Particles pseudotyped with SARS-COV2 Spike function in neutralization assays.**

423 HIV-1-Gluc particles were pseudotyped with SARS-COV2 Δ19 Spike (left) or SARS-COV2

424 R682Q Δ19 Spike (right). Plasma was obtained from two patients with a confirmed COVID-19

425 infection, or infection negative patients. Two-fold serially diluted plasma was incubated with

426 pseudotypes for 1 hour at 37C. The mixture was subsequently incubated with

427 293/ACE2/TMPRSS2 cells and Gluc measurements were taken 2 days post transduction.

428